Geophysical Journal International

*Geophys. J. Int.* (2016) **205,** 1196–1207
Advance Access publication 2016 March 1
GJI Gravity, geodesy and tides

doi: 10.1093/gji/ggw081

# AIUB-RL02: an improved time-series of monthly gravity fields from GRACE data

U. Meyer, A. Jäggi, Y. Jean and G. Beutler

*Astronomical Institute, University of Bern, Sidlerstrasse* 5, 3012 *Bern, Switzerland. E-mail: ulrich.meyer@aiub.unibe.ch*

Accepted 2016 February 25. Received 2016 February 24; in original form 2015 September 24

## SUMMARY

The new release AIUB-RL02 of monthly gravity models from GRACE GPS and K-Band range-rate data is based on reprocessed satellite orbits referring to the reference frame IGb08. The release is consistent with the IERS2010 conventions. Improvements with respect to its predecessor AIUB-RL01 include the use of reprocessed (RL02) GRACE observations, new atmosphere and ocean dealiasing products (RL05), an upgraded ocean tide model (EOT11A), and the interpolation of shallow ocean tides (admittances). The stochastic parametrization of AIUB-RL02 was adapted to include daily accelerometer scale factors, which drastically reduces spurious signal at the 161 d period in $C_{20}$ and at other low degree and order gravity field coefficients. Moreover, the correlation between the noise in the monthly gravity models and solar activity is considerably reduced in the new release. The signal and the noise content of the new AIUB-RL02 monthly gravity fields are studied and calibrated errors are derived from their non-secular and non-seasonal variability. The short-period time-variable signal over the oceans, mostly representing noise, is reduced by 50 per cent with respect to AIUB-RL01. Compared to the official GFZ-RL05a and CSR-RL05 monthly models, the AIUB-RL02 stands out by its low noise at high degrees, a fact emerging from the estimation of seasonal variations for selected river basins and of mass trends in polar regions. Two versions of the monthly AIUB-RL02 gravity models, with spherical harmonics resolution of degree and order 60 and 90, respectively, are available for the time period from March 2003 to March 2014 at the International Center for Global Earth Models or from ftp://ftp.unibe.ch/aiub/GRAVITY/GRACE (last accessed 22 March 2016).

**Key words:** Satellite geodesy; Time variable gravity; Global change from geodesy.

## 1 INTRODUCTION

The Gravity Recovery And Climate Experiment (GRACE; Tapley *et al.* 2004) has been in orbit for more than 13 yr. Its essential result is a time-series of monthly gravity field solutions of the Earth. The temporal variations observed in these gravity models over the continents are attributed to the hydrological cycle, ice mass changes in the polar and subpolar regions and large glaciers, and post-glacial rebound. Even local hydrological processes like draughts or major flooding events can be detected (e.g. Chen *et al.* 2010; Long *et al.* 2013). The temporal variations observed over the oceans are assessed, for example, by Chambers & Bonin (2012).

The GRACE monthly gravity models, denoted L2-products, are computed from pre-processed (L1B) GRACE observations including GPS observations, attitude data from the star cameras, non-gravitational accelerations measured onboard the GRACE satellites and the intersatellite range rates derived from the K-Band link between the two GRACE satellites (Dunn *et al.* 2003). The L1B data are available via web-interfaces at the Physical Oceanography Distributed Active Archive Center (PODAAC[1]) hosted at JPL or at the Information System and Data Center (ISDC[2]) hosted at GFZ. They have been completely reprocessed once during the mission time and the resulting L1B-RL02 is available since 2013.

To separate the gravity variations of interest from other time variable signals, a number of background models are applied during the L2-processing. These comprise ocean tides, as well as short period mass variations in the oceans and the atmosphere that are summed up, for example, in the dedicated atmosphere and ocean dealiasing (AOD1B) products. The AOD1B-products were reprocessed several times, the most recent version is RL05 (Flechtner & Dobslaw 2013).

The L2-products are provided by the official GRACE processing centres Center for Space Research (CSR; Bettadpur 2012) and the German Research Center for Geosciences (GFZ; Dahle *et al.* 2012),

[1] http://podaac.jpl.nasa.gov (last accessed 22 March 2016)
[2] http://isdc.gfz-potsdam.de (last accessed 22 March 2016)

while the Jet Propulsion Laboratory (JPL) computes L2-products for validation (Watkins & Yuan 2012). The most recent versions of gravity field products in all three cases are RL05. AOD1B and L2 gravity field products are also available at PODAAC or ISDC. Apart from the gravity fields mentioned above a number of alternative time-series of monthly or even sub-monthly solutions were produced by other institutions, e.g. the Astronomical Institute of the University of Bern (AIUB). For a complete overview we refer to the website of the International Center for Global Earth Models (ICGEM[3]).

AIUB has produced and released a first series of monthly GRACE gravity models AIUB-RL01 (Meyer *et al.* 2012), which were generated from L1B-RL01 data in 2011. The release of L1B-RL02, as well as several model updates, has made a reprocessing necessary. This opportunity was used to switch to the recent IERS conventions (Petit & Luzum 2010), to reprocessed GPS orbits from the Center for Orbit Determination in Europe (CODE; Dach *et al.* 2009), and to revisit the general processing strategy of the Celestial Mechanics Approach (CMA; Beutler *et al.* 2010a,b).

The quality of the monthly gravity models was significantly improved (relative to AIUB-RL01) and the spectral resolution was increased to the spherical harmonic degree and order 90. The new release AIUB-RL02 of monthly gravity models will contribute to combined monthly models in the frame of the European Gravity Service for Improved Emergency Management (EGSIEM; Jäggi *et al.* 2015) project, where AIUB is in charge of the combination of monthly models from several processing centres to implement the prototype of a future gravity field service.

In Section 2, the changes from AIUB-RL01 to RL02 related to the reprocessed observation data and model updates are listed and the specific impact on the resulting gravity field solutions is detailed. In Section 3, the new processing strategy and stochastic parametrization is discussed in detail. In Section 4, calibrated errors are derived and the signal content in the monthly gravity models is discussed. The monthly gravity models are validated in Section 5 by comparison to the official GFZ-RL05a and CSR-RL05 products. To this end seasonal variations in major river basins and mass trends in Antarctica are evaluated. In Section 6, the findings are summarized and an outlook on future plans is given.

## 2 OBSERVATIONS AND BACKGROUND MODELS

The CMA treats gravity field estimation as a generalized orbit determination problem. It is based on a reduced dynamic orbit representation using pseudo-stochastic orbit modelling, that is, constrained stochastic accelerations at short intervals in all three directions of the local orbital frame (Jäggi *et al.* 2006). The CMA has been used to derive static GRACE gravity fields (e.g. Jäggi *et al.* 2010, 2011a), its application to monthly GRACE gravity field models AIUB-RL01 is provided in Meyer *et al.* (2012).

AIUB-RL01 was already outdated in 2013, when the complete L1B data were reprocessed. The most important improvement of L1B-RL02 relative to previous releases is the recomputed K-Band attitude correction that compensates geometric biases due to misalignment of the two GRACE satellites (Horwath *et al.* 2011). The attitude data show small differences, as well.

To test the new L1B-RL02 data, monthly solutions of the two years, 2007 and 2008, were reprocessed. The effect on the monthly

[3] http://icgem.gfz-potsdam.de (last accessed 22 March 2016)

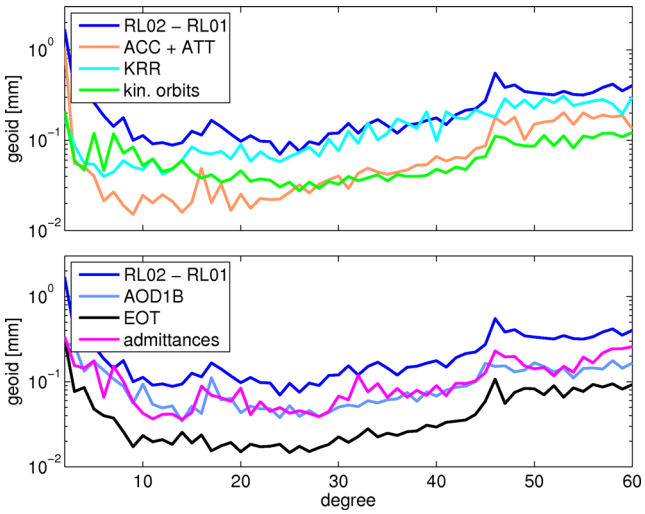


**Figure 1.** Difference degree amplitudes between an AIUB-RL02 and RL01 monthly solution (09/2007) and between RL02 and several test solutions where one of the improvements from RL01 to RL02 was undone.

gravity field solutions turned out to be very small, about one order of magnitude below the level of variability of the solutions. Subsequently, the noise level of the monthly solutions could be lowered by a number of other improvements and the tests were repeated in a way that only one of the changes from AIUB-RL01 to -RL02 is undone at a time while the rest of the improvements stay active to keep the noise level down.

The effect of individual changes from AIUB-RL01 to RL02 is evaluated in Fig. 1 for a test month (September 2007) in terms of difference degree amplitudes between a monthly solution with and without a specific L1B data (top) or background model (bottom) update. The difference degree amplitudes between AIUB-RL01 and -RL02 are also provided for reference.

For all comparisons in this and the following sections, a special version of AIUB-RL01 complete to degree and order 60 was computed (the official RL01 was truncated at degree 60 and order 45). AIUB-RL02 was produced in two different versions: one up to degree and order 60, the other up to degree and order 90. For all comparisons to AIUB-RL01 the version up to degree 60 was used. Where the maximum degree is not obvious from the context it is added to the label.

The differences between AIUB-RL01 and -RL02 (dark blue) are of the same magnitude or even bigger than the noise level of RL02 (see Fig. 9). As expected, the effect of the change in the K-Band attitude correction (light blue) is most important but also the changes in the accelerometer and attitude observations (orange) reach a substantial level, especially at high degrees ($l > 40$). Accelerometer and attitude data were tested together because in our processing the accelerations are rotated to the orbital frame in an external preprocessing step and the effects cannot be separated later.

After the change to L1B-RL02, all background models were updated to the most recent versions. The atmosphere and ocean dealiasing product is updated from RL04, used in AIUB-RL01, to RL05 (Flechtner & Dobslaw 2013). The effect on the gravity field (steel blue) is well below that of the corrected geometric K-Band biases (light blue) but still at a significant level. The update from ocean tide model EOT08A to EOT11A (Savcenko & Bosch 2011) does not lead to a significant improvement (black). This was

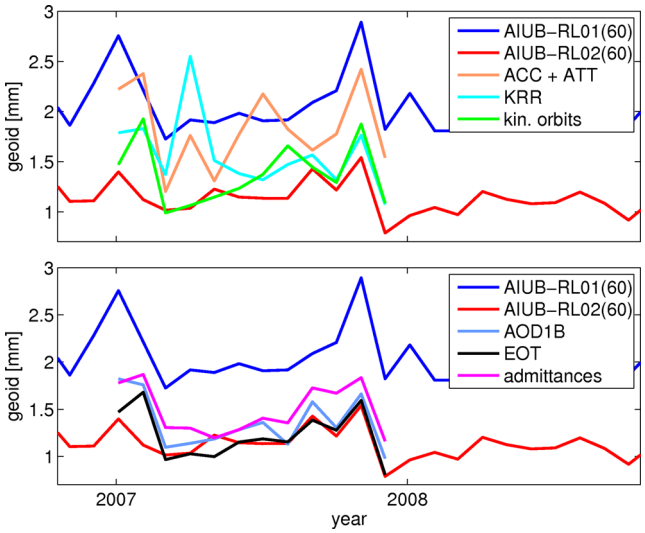


**Figure 2.** Noise over the oceans for 12 monthly solutions in 2007 of AIUB-RL01(60), AIUB-RL02(60), and several test solutions where one of the improvements from RL01 to RL02 was undone. Top: reprocessed observations, bottom: updated background models.

expected because the changes from EOT08A to EOT11A are of local nature.

The incorporation of shallow tides (admittances), linearly interpolated from the main tides of EOT11A (T. Mayer-Gürr, personal communication, 2013), turned out to be a major step forward (magenta). The effect is of comparable magnitude to that of the change of the AOD1B-products (steel blue).

Finally, the kinematic orbits of the GRACE satellites, which are determined in a precise point positioning from the GPS phase observations, were recomputed. They enter gravity field processing as pseudo-observations (Jäggi *et al.* 2011b). The new kinematic orbits rely on reprocessed GPS orbits from the CODE analysis centre (Steigenberger *et al.* 2011) and are based on the IERS conventions from 2010 (Petit & Luzum 2010) and no longer on the 2003 conventions (McCarthy & Petit 2003). In the process of kinematic orbit determination maps of the empirical phase center variation of the GRACE GPS antennas (Jäggi *et al.* 2009) were re-estimated.

The effect of the new kinematic orbits (green) is most significant at the very low degrees, as it can be expected due to the limited sensitivity of the GPS-derived positions to the gravity field at higher degrees. However, it stays at a level one order below that of the time-variable gravity signal (see Fig. 9).

Fig. 1 visualizes the size of the separate effects but does not tell whether they really are improvements. Therefore we have to estimate the noise in the monthly gravity models. The noise in the monthly solutions may be evaluated by the temporal variations over the oceans, where no signal of hydrological origin is expected. The differences between the monthly solution and a static field are computed on a grid with a cell size of 3°, corresponding to a spherical harmonic expansion up to degree and order 60, secular and seasonal variations are fitted to all grid cells and subtracted to remove long-periodic signals of oceanic origin, the grid cells are weighted by the cosine of the latitude to account for their different sizes and the standard deviation over all ocean cells is computed. To avoid leakage from the continents the shoreline is shifted by three grid cells (i.e. 9°) into the oceans.

Fig. 2 shows the standard deviations computed in this way for all monthly solutions in 2007. The decrease of noise level from AIUB-RL01 (blue) to -RL02 (red), both estimated up to degree and order 60, is clearly visible. The changes from RL01 to RL02 were undone one by one and the effect on the noise level is studied. The reprocessed accelerometer and attitude data (orange) seem to play the most important role while the correction of the geometric K-Band biases in L1B-RL02 (light blue), the update of the AOD1B product from RL04 to RL05 (steel blue), the implementation of shallow tides (magenta) and the reprocessing of the kinematic orbits (green) all take a considerable share in the reduction of noise. The change of the ocean tide model (black) once more only plays a minor role.

The screening of the L1B observations was done separately for the AIUB-RL01 and -RL02 solutions. Bad observations in L1B-RL01 which were removed in AIUB-RL01 may be usable in the reprocessed L1B-RL02. On the other hand, some data gaps in L1B-RL01, which were caused by L1B pre-processing problems were filled in L1B-RL02, but not all of the added observations are good enough for L2-processing. They therefore have to be screened out for AIUB-RL02. The screening differences also cause differences between AIUB-RL01 and -RL02.

For Fig. 2 (top), strictly speaking a dedicated screening should have been performed for each of the test solutions because L1B-RL01 and -RL02 data were mixed. This was not done and all solutions were determined using the final RL02 screening tables. The outlier in the KRR-test visible in Fig. 2 (top) in April 2007 is caused by bad observations and the strong impact of the choice of either L1B-RL01 or -RL02 attitude and accelerometer data has also to be attributed at least partially to screening issues. The test month underlying Fig. 1 was chosen not to be afflicted by this kind of problem.

The data, models and conventions applied for AIUB-RL02 are summarized in Table 1. The choice of the *a priori* gravity field model is only added for the sake of completeness. Due to the parametrization of the CMA the *a priori* gravity field and its *a priori* temporal variations only play a minor and indirect role for the estimated gravity field coefficients (Meyer *et al.* 2015a).

## 3 PROCESSING STRATEGY AND PARAMETRIZATION

The parametrization of AIUB-RL01 has been revisited to optimally fit the improved accuracy of the updated models and L1B-RL02 data. The satellite orbits are processed in daily arcs. For each arc initial conditions, stochastic accelerations (see Table 2), and accelerometer scale factors are estimated. The spherical harmonic coefficients (SHCs) of the gravity field are set up together with the arc-specific parameters. The daily Normal EQuations (NEQs) with respect to the kinematic orbits of GRACE A, B, and with respect to the K-Band range-rate observations are combined and the arc-specific parameters are pre-eliminated from the combined NEQs. Finally, the reduced NEQs are accumulated to monthly batches to solve for the gravity model parameters.

For the computation of AIUB-RL01 the non-gravitational accelerometer observations in cross-track direction were not used due to their bad signal-to-noise ratio. The omitted signal could be absorbed by the stochastic piecewise constant accelerations and additional periodic 1/rev-accelerations in all three directions estimated once per arc. For AIUB-RL02 this strategy was changed. The observed cross-track accelerations are now used but the periodic 1/rev-accelerations became obsolete.

**Table 1.** AIUB-RL02 is based on the following input data, background models and conventions. Numbers in brackets indicate the maximum applied degree and order of a model given in spherical harmonic coefficients (SHC).

| | Data or model used | Reference |
|---|---|---|
| Observation data | L1B-RL02 | |
| Reference frame | ITRF2008, realized by IGb08 | Altamimi *et al.* (2011) |
| Conventions | IERS2010 | Petit & Luzum (2010) |
| GPS orbits | Reprocessed | Steigenberger *et al.* (2011) |
| PCV corrections | Determined from red. dyn. orbits | Jäggi *et al.* (2009) |
| AOD1B | RL05 (100) | Flechtner & Dobslaw (2013) |
| Ocean tides | EOT11A (100) | Savcenko & Bosch (2011) |
| | Transformed to SHC | e.g. Mayer-Gürr *et al.* (2011) |
| Complemented by | $M_{tm}$, $M_{sqm}$ (FES2004) | Lyard *et al.* (2006) |
| | $\Omega_{1,2}$, Sa, Ssa: (HW95) | Hartmann & Wenzel (1995) |
| Admittances | Interpolated linearly | Mayer-Gürr, personal communication (2013) |
| Atmospheric tides | As included in AOD1B | |
| *A priori* gravity | AIUB-GRACE03S (160) | In-house |
| *A priori* variations | Secular, annual, semi-annual (30) | In-house |
| Third bodies | Sun, moon, selected planets (1) | DE 421 |
| Solid Earth tides | IERS2010 | Petit & Luzum (2010) |
| Earth pole tide | IERS2010 | Petit & Luzum (2010) |
| Ocean pole tide | Desai (100) | Petit & Luzum (2010) |

**Table 2.** Stochastic accelerations estimated for AIUB-RL02.

| | Bias | Third-order polynomial | Piecewise constant accelerations |
|---|---|---|---|
| Radial | 24 h | – | 15 min |
| Along-track | – | 24 h | 15 min |
| Cross-track | 24 h | – | 15 min |

The daily constant accelerations shall absorb the unknown accelerometer biases. The daily averages of the piecewise constant accelerations are constrained to 0 to avoid a singularity due to the daily constant accelerometer biases. The third-order polynomial in along-track turned out to be helpful to model slow variations in the corresponding accelerometer bias. These occur, for example, whenever the temperature at the satellites is not constant (when the heaters are switched off, the cooling of the satellites is a non-linear process that takes several days; the same is true for the warming-up when the heaters are turned back on).

When the normal equations of GRACE A and B are combined, the piecewise constant accelerations are transformed to the mean of the corresponding accelerations of both satellites and half of their difference due to numerical reasons (Beutler *et al.* 2010a). The absolute part is constrained to 0 with a standard deviation of $3 \times 10^{-9}\,\mathrm{m\,s^{-2}}$ while the differential part is constrained 100 times stronger, also to 0, to account for the stupendous accuracy of the K-Band observations (Beutler *et al.* 2010b).

The *a priori* sigma of unit weight applied to the K-Band range-rate measurements is $3 \times 10^{-7}\,\mathrm{m\,s^{-1}}$, the one applied to the carrier phase GPS observations used to derive kinematic positions is $2 \times 10^{-3}$ m. Both values are based on the analysis of the corresponding residuals (the daily root-mean-square (RMS) of the range-rate residuals varies between $1.5 \times 10^{-7}$ and $3.5 \times 10^{-7}\,\mathrm{m\,s^{-1}}$ depending mainly on the intersatellite distance). For the combination of the normal equations resulting from the kinematic orbits and from the K-Band range rates a relative weight of GPS of the order of $(3 \times 10^{-7})^2/(2 \times 10^{-3})^2 = 2.25 \times 10^{-8}$ therefore seems to be appropriate. Experiments showed, however, that a value of $1 \times 10^{-10}$ leads to much better results. The reason, why GPS has to be downweighted by a factor of more than 200 is not clear.

Data screening is done semi-automatically. First, *a priori* orbits are determined including loosely constrained stochastic parameters. These are based on a recent *a priori* gravity model up to high degree and including time variations. The K-Band range-rate residuals are screened manually, taking also the GRACE Sequence Of Events file into account. Periods of dubious data quality are excluded by a gap-table that is automatically read during further processing. The procedure is iterated until all range-rate residuals seam acceptable in size. We refrain from a fully automated screening algorithm because steep gradients of the gravity potential along the satellite's path may lead to sharp peaks in the range-rate residuals of the *a priori* orbits.

A second screening is performed when the daily NEQs containing the gravity field parameters are accumulated to monthly NEQs and solved. For each month 30 or 31 different solutions are computed, where in each of the solutions one of the days of the month is left out. A comparison of the solutions clearly shows faulty days that may be revisited in the first screening step or excluded from the final monthly solution. Tables of the days used are included in the headers of the monthly solution-files provided via ICGEM.

AIUB-RL02 is based on a common estimation of orbits and gravity field parameters. Experiments with a separate estimation are described in Meyer *et al.* (2015a). A significant reduction of noise can be achieved using a separate estimation, but at the expense of signal attenuation, caused by absorption by the stochastic accelerations (Meyer *et al.* 2015b).

A preliminary version AIUB-RL02p of monthly models was computed without estimation of accelerometer scale factors. The results in terms of noise, that is, standard deviations of variability over the oceans, are shown in Fig. 3 where the performance of AIUB-RL02p (green), solved up to degree and order 60, is compared to that of GFZ-RL05a (magenta), also a reduced version solved only to degree 60, and to CSR-RL05 (black). Degree 1 coefficients and $C_{20}$ are excluded from this evaluation because they are not well determined from GRACE data alone. The daily solar flux values (blue) and their 30 d sliding mean (red) are also provided in Fig. 3.

The correlation between noise and solar activity (Table 3) is striking. In all cases the significance of correlation is at the 0.0001 confidence level. AIUB-RL02p and GFZ-RL05a seem to suffer

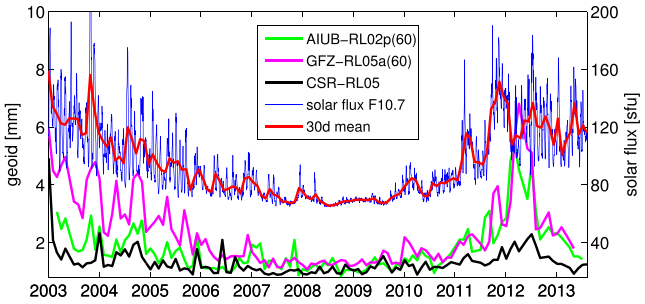


**Figure 3.** Noise of monthly solutions over the oceans in relation to the solar flux.

in particular from increased solar activity. No accelerometer scale factors are estimated for GFZ-RL05a and AIUB-RL02p, in contrast to CSR-RL05 (and AIUB-RL02, see below). Note that the peaks in the noise in 2012 are not related to solar activity but to a 3 d orbit repeat cycle.

The introduction of 3-hourly accelerometer scale factors drastically reduced the dependence of GFZ-RL05a on solar activity (Dahle *et al.*, in preparation). A similar effect could be observed for AIUB-RL02, as well, by the introduction of daily accelerometer scale factors. The scale factors were set up in all three directions in the orbital frame, but the main effect is related to the scale factors in along-track. Consistency with a static gravity model is significantly improved (Fig. 4). The gain in consistency is most obvious during times of high solar activity, see Fig. 4 (top), and much less pronounced during times of quiet ionosphere conditions, see Fig. 4 (bottom).

Evaluating the noise of the monthly gravity models in terms of standard variations of the short periodic variability over the oceans (Fig. 5), the quality of AIUB-RL02 (red) is close to that of CSR-RL05 (black). It is worth-while to note that the main effect of the accelerometer scale factors consists of a reduction of spurious 161 d variations in the SHC $C_{20}$, excluded in Figs 3 and 5. Time-series of the $C_{20}$-coefficient are shown in Fig. 6. The mean of the monthly $C_{20}$-values of CSR-RL05 was subtracted to center all time-series around 0. The reduction in spurious variability on 161 d period from AIUB-RL01 (blue) to -RL02p (green) is due to the improvement of the background modelling. The reduction from AIUB-RL02p (green) to -RL02 (red) is due to the estimation of daily accelerometer scale factors.

The 161 d cycle corresponds to the time it takes the orbital plane of the GRACE satellites to rotate by 180°. The angle between the normal to the orbital plane and the direction to the sun therefore also varies by 180° within 161 d. Related to this effect is also the aliasing frequency of 161 d of the S2-tide on GRACE observations. It cannot yet be decided whether the observed effect on the monthly gravity models is due to a direct effect of the sun or the ionosphere on the GRACE observations or an aliasing effect of the S2-tide. The small bias between $C_{20}$-values derived from GRACE (CSR-RL05, black, or AIUB-RL02, red) or from LAGEOS Satellite Laser Ranging (SLR) observations (magenta) that is visible in Fig. 6 is not yet explained either.

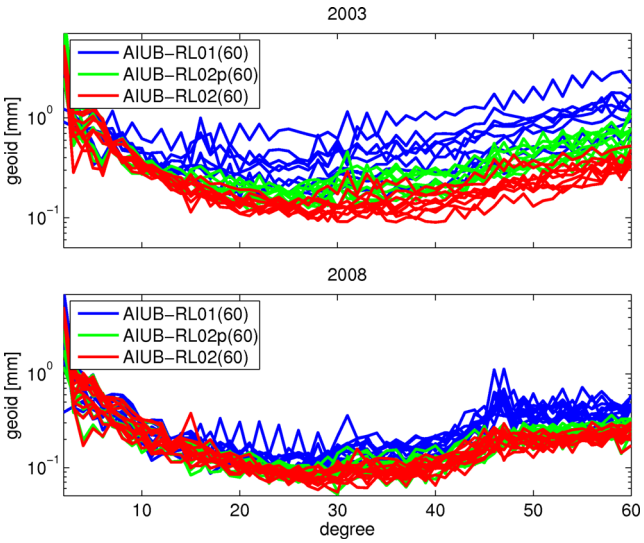


**Figure 4.** Difference degree amplitudes between different releases of monthly gravity fields and the static part of AIUB-GRACE03S. Shown are the years 2003 (top, high ionosphere activity) and 2008 (bottom, quiet ionosphere conditions).

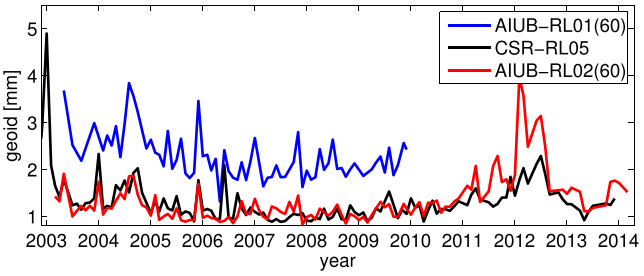


**Figure 5.** Noise in monthly models in terms of the standard deviations of the variability over the oceans.

## 4 CALIBRATED ERRORS AND OPTIMAL RESOLUTION OF MONTHLY FIELDS

The formal errors provided with the monthly AIUB-RL02 gravity models, see Fig. 8 (top), mainly depend on the observation geometry, that is, on orbit geometry and availability of observations. To derive more realistic error estimates one may look at the variability of the SHC with time (Schmidt *et al.* 2007). To reduce

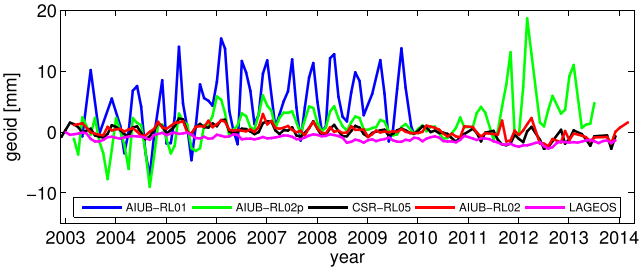


**Figure 6.** Effect of accelerometer scale factors on $C_{20}$ and comparison to CSR-RL05 and LAGEOS derived values.

**Table 3.** Correlation between noise in 116 monthly gravity fields and the 30 d mean of solar flux evaluated at the epochs of the monthly solutions.

| | GFZ-RL05a(60) | AIUB-RL02p(60) | CSR-RL05(60) | AIUB-RL02(60) |
|---|---|---|---|---|
| Correlation coefficient | 0.75 | 0.68 | 0.62 | 0.55 |

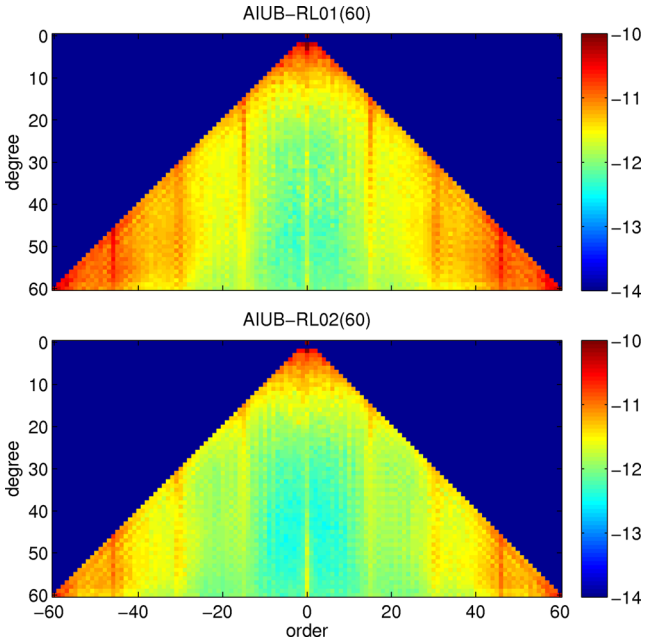


**Figure 7.** Calibrated errors per coefficient of AIUB-RL01(60) (top) and AIUB-RL02(60) (bottom), derived from the variability of the monthly solutions over the oceans (trends and seasonal variations subtracted).

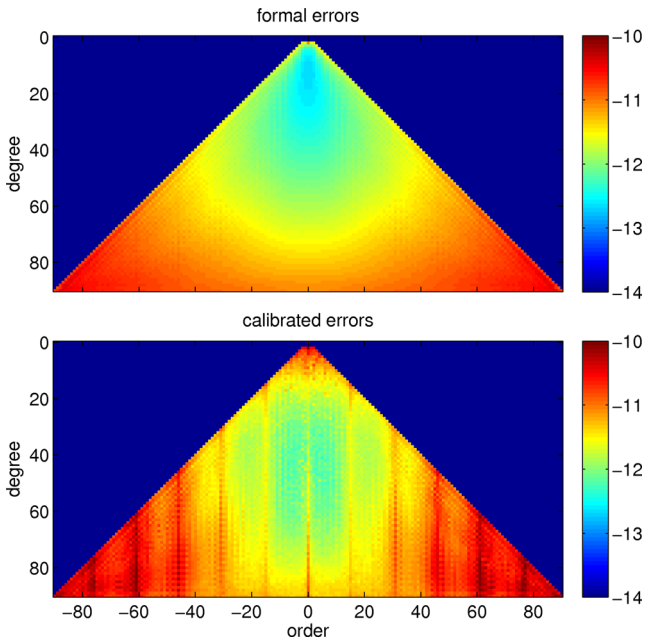


**Figure 8.** Mean formal errors per coefficient of AIUB-RL02 monthly solutions (top) and calibrated errors (bottom). S-coefficients on the left, C-coefficients on the right side of the triangle plot.

misinterpretation of seasonal gravity variations as noise, either the inter-annual variability of monthly solutions is evaluated, or the secular and seasonal variations are approximated by a deterministic model to the SHC and subtracted from the monthly gravity models.

Following the latter approach calibrated errors were derived from monthly AIUB-RL01 (Fig. 7, top) and AIUB-RL02 (Fig. 7, bottom). In both cases the monthly models up to degree and order 60 were used. The reduction in noise from AIUB-RL01 to -RL02 is obvious. While the coefficients beyond order 45 where not estimated in the final AIUB-RL01 models, because they were anyway dominated by noise, such a measure is not justified any more in AIUB-RL02.

The increased variability at low degree coefficients is at least partly caused by the gravity variations exceeding our simple deterministic model, which assumes a constant amplitude of annual and semi-annual variations. The calibrated errors therefore are pessimistic estimates. The vertical stripes in Fig. 7 are related to zonal coefficients and resonant orders, which are subject to spectral aliasing with geophysical background model errors (Seo *et al.* 2008).

The calibration of errors is repeated for the final AIUB-RL02 solutions to full degree and order 90 (Fig. 8, bottom). The general pattern of the calibrated errors resembles that of the formal errors (Fig. 8, top). However, the stripes at zonal coefficients and resonant orders disturb the picture. For high degrees and low orders the calibrated errors seem to be even smaller than the formal ones, while at high degrees and high orders the formal errors are definitely optimistic.

The variability of the monthly solutions in difference degree amplitudes relative to AIUB-GRACE03S and the corresponding formal and calibrated errors are presented in Fig. 9, which shows the mean of the difference degree amplitudes over all months (red) and their mean formal errors (light blue). The secular and seasonal variations are modelled and subtracted from the monthly gravity fields. The calibrated errors (magenta) are derived from the remaining temporal variability. They slightly differ from the difference degree amplitudes of the reduced monthly solutions (dark blue), because coefficient-wise biases were estimated. If the reference epoch of

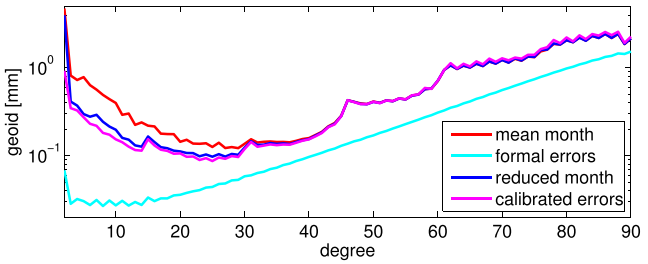


**Figure 9.** Difference degree amplitudes of AIUB-RL02 relative to AIUB-GRACE03S prior (mean month) and after subtraction of modelled time variations (reduced month), mean of the formal errors over all months and calibrated errors.

the trend-estimates refers to the mean epoch of the time-series of monthly fields, if furthermore the time-series is free of gaps and if it comprises an integer number of cycles of seasonal variations, then these biases vanish and the calibrated errors perfectly match the difference degree amplitudes of the reduced months.

The orderwise striping is also present in the quotient of the calibrated and the formal errors. This fact leads to the idea of orderwise calibration factors, calculated as the mean over all quotients of the same order (Fig. 10). The coefficients of low degree $l$ and order $m$

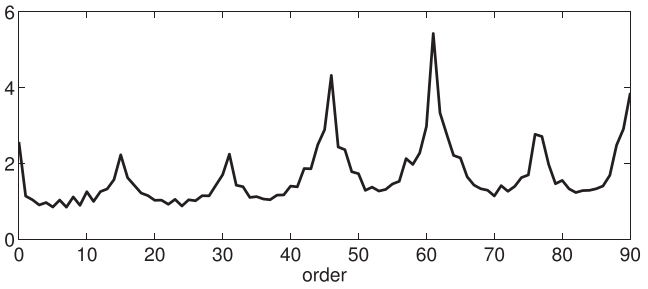


**Figure 10.** Orderwise calibration factors for formal errors of spherical harmonic gravity field coefficients of AIUB-RL02.

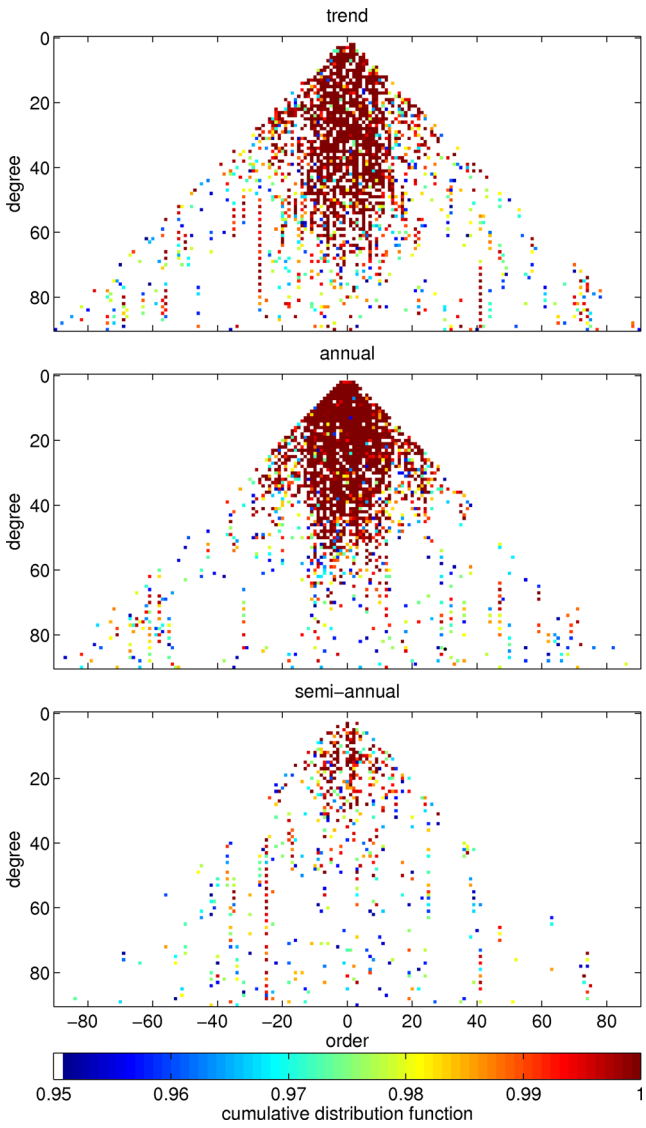


**Figure 11.** Significance of trends (top), annual (middle) or semi-annual (bottom) variations fitted to AIUB-RL02.

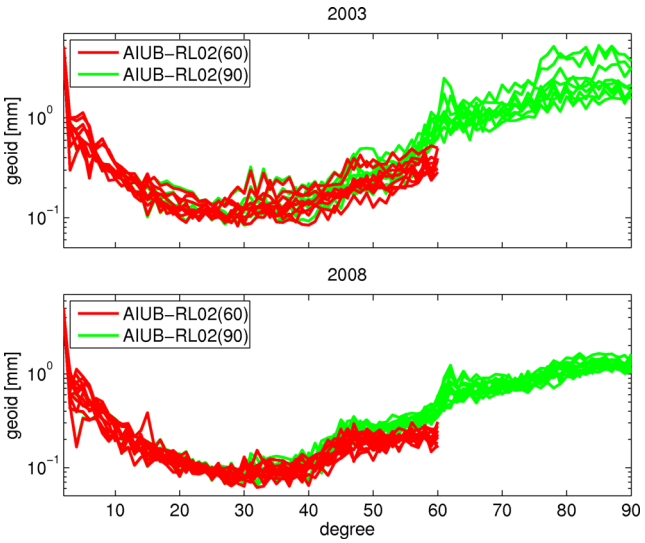


**Figure 12.** Difference degree amplitudes between monthly AIUB-RL02 gravity fields from 2003 (top) or 2008 (bottom) and the static model AIUB-GRACE03S.

(i.e. where $l + m < 31$) are excluded, because their variability is dominated by non-seasonal signals. These calibration factors may be used to scale the formal errors, which are provided with the monthly AIUB-RL02 coefficients.

In the next step, the signal content of the AIUB-RL02 monthly gravity fields is assessed. The major time-variable signal expected in the SHC is a seasonal variation due to the hydrological cycle, as well as a secular trend due to ice mass changes in glaciated regions and due to GIA. The latter two effects cannot be separated easily in the spectral domain.

We therefore assess the signal content in the monthly models by a test of significance of secular or seasonal variations fitted to the time-series of monthly SHC. This particular significance test was introduced by Davis *et al.* (2008) who applied it to filter the SHC of the monthly models. Fig. 11 shows the results for secular, annual and semi-annual variations, fitted to monthly solutions from 2003 to 2009. Comparing Fig. 11 to the corresponding results for AIUB-RL01 (Meyer *et al.* 2012) the increased sensitivity, or reduced noise, of AIUB-RL02 becomes obvious. For better comparison the time period of AIUB-RL02 tested for significance was adjusted to that of the availability of RL01.

From the analysis of the calibrated errors and the sensitivity to temporal variations as visualized by the significance tests one might conclude to truncate the solution space of AIUB-RL02 somewhere beyond degree 75, where not much secular or seasonal signal could be retrieved, and at resonant order 61, where the calibrated errors show predominantly noise. But this measure would hinder a direct comparison with other monthly gravity field releases, which nowadays are available at least up to degree and order 90 (such as GFZ-RL05a, CSR-RL05(96), JPL-RL05). Moreover, and what is more important, the combinability with other monthly solutions, which is a major goal of the EGSIEM project, would also suffer.

Therefore, AIUB-RL02 is made available up to degree and order 90. This extension of the solution space goes hand in hand with a loss of precision for a part of the spherical harmonic spectrum as visualized by Fig. 12. Fig. 12 (top) represents a time span where the monthly solutions suffer from strong solar activity (2003), while Fig. 12 (bottom) refers to a quiet period (2008).

Up to degree 30 the differences to the static model are dominated by signal in the monthly solutions. The signal content in the degree 60 and the degree 90 solutions agrees well during both example periods. Above degree 30 the difference degree amplitudes are impaired by noise in the monthly solutions. Especially when noise levels are generally low during the minimum of the solar cycle in 2008 an increase in the noise level of the coefficients from degree 30 to 60 becomes visible due to the extension of the solution space to degree and order 90. Because most users apply some type of degree-dependent smoothing, e.g. a Gauss-type filter, this increase in noise beyond degree 30 may be accepted. It was nevertheless decided to also provide alternative AIUB-RL02 solutions up to degree and order 60.

Peaks may be observed in Fig. 12, which are accompanied by a general rise beyond the specific degree in the difference degree amplitudes at degrees 16, 31, 46, 61 and 76. This phenomenon is due to the increased noise level at the corresponding resonant orders, as visible in Fig. 8 (bottom). All degree variances including a specific resonant order suffer from the noise in the coefficients of that order.

**Table 4.** Variability of estimated annual amplitudes or trends over the oceans in terms of weighted standard deviations.

| | AIUB-RL01(60) | AIUB-RL02(60) | CSR-RL05(60) | GFZ-RL05a(60) |
|---|---|---|---|---|
| Annual variations [cm] | 5.7 | 2.3 | 2.4 | 5.0 |
| Trends [cm a$^{-1}$] | 3.0 | 1.5 | 1.7 | 3.2 |

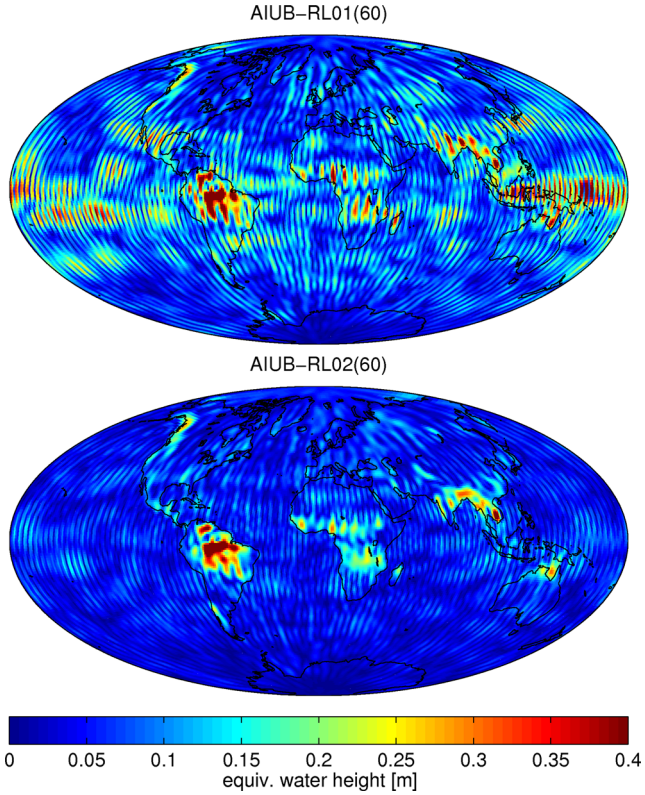


**Figure 13.** Amplitudes of annual variations in equivalent water height, derived from AIUB-RL01(60) (top) and AIUB-RL02(60) (bottom). No smoothing is applied.

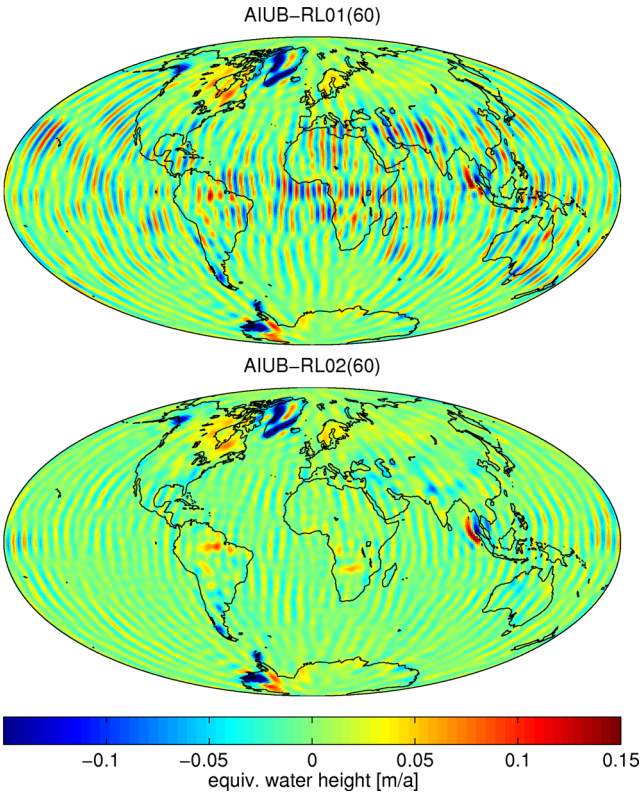


**Figure 14.** Trends in equivalent water height determined from 7 yr of AIUB-RL01(60) (top) and AIUB-RL02(60) (bottom) monthly solutions. No smoothing applied.

## 5 EVALUATION OF AIUB-RL02

The major improvements from AIUB-RL01 to RL02 consist of a reduction of noise due to the reprocessed input data, the modified parametrization, and a better separation of time-variable signal due to updated background models. In this section, we focus on the seasonal variations due to the hydrological cycle and the trends in ice mass deduced from the time-series of monthly models. Degree 1 coefficients and $C_{20}$ are excluded from the analysis. We recommend to replace these coefficients in all monthly GRACE gravity fields by the SLR-derived values.

The monthly sets of SHC are scaled to equivalent water heights (e.g. Swenson & Wahr 2002) and transformed to grids by spherical harmonic synthesis. Annual, semi-annual and secular variations are fitted to the time-series of each of the grid cells. The resulting amplitudes are shown in Fig. 13 for AIUB-RL01(60) (top) and for AIUB-RL02(60) (bottom). In both cases a time span of 7 yr (2003–2009) was evaluated. All comparisons shown in this section refer to this time span which corresponds to the availability of AIUB-RL01.

The spots and stripes over the ocean may be taken as an indication of the noise in the solution. The standard deviations over all ocean grid cells, weighted by the cosine of the latitude, are shown in Table 4. They confirm the significant reduction of noise in Fig. 13. For comparison, the official CSR-RL05(60) and a special version of GFZ-RL05a, estimated to a maximum degree and order of 60, were evaluated.

A comparable reduction of noise may be observed for the secular trends derived from AIUB-RL01(60) or -RL02(60), see Fig. 14 (top) and (bottom). The corresponding standard deviations over the oceans are included in Table 4, again with CSR-RL05(60) and GFZ-RL05a(60) for comparison.

No smoothing was applied in Figs 13 and 14 and for the computation of the standard deviations over the oceans. Note that no correction was applied to compensate the effect of the Sumatra–Andaman earthquake in December 2004. It is therefore visible as an apparent trend in Fig. 14.

From monthly grids of equivalent water height the mean water heights within specific river basins may be computed on a monthly basis. The river basin masks were obtained from the model Total Runoff Integrating Pathways (TRIP[4]). The results derived from AIUB-RL02(60) for selected river basins are shown in Fig. 15. Again no smoothing was applied. Periods with increased scatter in June to November 2004 and April to August 2012 are related to weak observation geometry due to orbit resonance.

[4] http://hydro.iis.u-tokyo.ac.jp/~taikan/TRIPDATA/TRIPDATA.html (last accessed 22 March 2016)

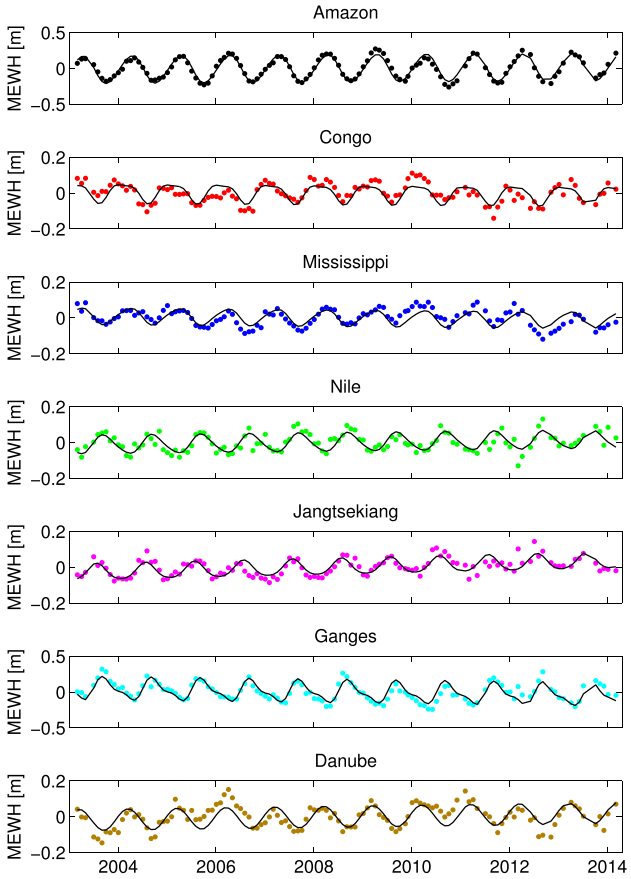


**Figure 15.** Variations in mean equivalent water height for major river basins, derived from AIUB-RL02(60). No smoothing applied.

To quantify the changes from AIUB-RL01 to -RL02 a deterministic model containing offset, trend, annual, and semi-annual variations was fitted to the mass changes within the river basins and is also included in Fig. 15 (black line). The annual amplitudes including error estimates as well as the residual RMS after removing bias, trend, annual and semi-annual variations are provided in Tables 5 and 6 for the original and smoothed gravity fields. To get comparable results only data from 2003 to 2009, where AIUB-RL01 is available, were used. CSR-RL05 and GFZ-RL05a are included for comparison. The monthly solutions up to degree and order 90 were processed, as well. For this purpose CSR-RL05(96) was truncated at degree and order 90.

AIUB-RL02 seems to contain more signal than RL01: the annual amplitudes are slightly larger, except for the Nile basin. The formal errors of the annual amplitudes decrease significantly from AIUB-RL01(60) to RL02(60) and this decrease in noise is also visible in the residual RMS (Table 6). The amplitudes agree well within the error bounds with CSR-RL05 and GFZ-RL05a. The unfiltered AIUB-RL02(90) suffer from high frequency noise, as is indicated by the formal errors of the annual amplitudes for the smaller basins or by the residual RMS, and need to be smoothed. The same is true for CSR-RL05(96), truncated at degree 90, and GFZ-RL05a(90). Compared to the two official releases of GRACE monthly gravity fields AIUB-RL02(90) stands out by its comparably lower noise, as indicated by the smaller standard deviations and the residual RMS (again with the exception of Nile).

After application of a 300 km Gauss filter (e.g. Wahr *et al.* 1998) the formal errors of the amplitudes derived from the different time-series are reduced to approximately the same level. The same is true for the residual RMS. This impressively illustrates the effectiveness of the filter. But the amplitudes are reduced by the filter by up to 15 per cent, as well.

The comparable performance of the degree 60 and degree 90 solutions when applying Gauss-smoothing may be explained by the characteristics of the filter. Only 0.7 per cent, calculated by the cumulative sum of all weighting factors, of the total signal remains in degrees higher than 60 after applying a 300 km Gauss filter. This approximation is based on the assumption of equal distribution of signal over all degrees. Actually the contribution of the high degree coefficients will be even smaller because the main part of the signal is contained in the low degree coefficients.

Mass trends are determined for Antarctica to quantify the quality gain from AIUB-RL01 to -RL02 in polar regions. As a first step, mass trends, together with seasonal variations, are estimated on a 1°-grid from the monthly models of 2003 to 2009 (see Fig. 16 for AIUB-RL02). Note that the size of the 1° grid cells varies with latitude and diminishes towards the poles, therefore not much signal is visible in Fig. 16 for the innermost part of Antarctica. No smoothing filter was applied.

The mass variations are integrated over basins. The basic definition of the Antarctic basins is taken from the Goddard Space Flight Center (GSFC) website on ICESAT[5]. Subsequently, the smaller basins are merged to larger units to best fit the basin definition in Horwath & Dietrich (2009).

The basin definition and the trend estimates derived from AIUB-RL02 are illustrated in Fig. 17. Fig. 18 shows the temporal variations within the three basins at the West coast of Antarctica with the most significant mass loss (red). In analogy to the river basins a deterministic model including bias, trend, annual and semi-annual variations is fitted to the monthly mass estimates within the basins (black). The main feature is a linear trend. As opposed to Fig. 15 the deviations from the model are not governed by noise. As already mentioned by Velicogna (2009), the mass loss in polar regions is accelerating. The model can be significantly improved by adding a quadratic term (green). The linear trend including the standard deviations and the residual RMS after removing bias, linear trend, quadratic trend, annual and semi-annual variations are provided in detail in Table 7 for AIUB-RL01, AIUB-RL02, CSR-RL05 and GFZ-RL05a. The gravity fields up to degree 60 or 90 were evaluated separately and the analysis was repeated, applying a 300 km Gauss filter.

In analogy to the river basins a significant quality gain occurred from AIUB-RL01 to -RL02, as can be seen from the standard variations or from the residual RMS. The AIUB-RL02 monthly gravity fields stand out with their low noise compared to the official releases of monthly models. This characteristic is best visible for the degree and order 90 gravity fields, except for basin 13, where CSR-RL05(60) shows the best performance after smoothing.

In case of basin 13, the unsmoothed trend estimates of AIUB-RL02(90), CSR-RL05(90) and GFZ-RL05a(90) show large discrepancies. These discrepancies go hand in hand with significantly increased formal errors and residual RMS. The increased scatter of basin 13 is also visible in Fig. 18. For large basins or basins which are predominantly East-West orientated the noise averages out when computing the ice mass per basin. Thus reliable trend

[5] http://icesat4.gsfc.nasa.gov/cryo_data/ant_grn_drainage_systems.php (last accessed 22 March 2016)

**Table 5.** Amplitude of annual mass variations in major river basins in centimetre of equivalent water height.

| | Gravity model | Amazon | Congo | Mississippi | Nile | Jangtsekiang | Ganges | Danube |
|---|---|---|---|---|---|---|---|---|
| No smoothing | AIUB-RL01(60) | 18.9 ± 1.2 | 4.0 ± 1.2 | 3.9 ± 1.2 | 5.4 ± 1.6 | 3.3 ± 1.2 | 11.8 ± 1.9 | 5.2 ± 1.9 |
| | AIUB-RL02(60) | 19.1 ± 1.1 | 4.8 ± 1.1 | 4.3 ± 1.0 | 4.9 ± 1.0 | 4.8 ± 0.9 | 13.1 ± 1.6 | 5.9 ± 1.5 |
| | CSR-RL05(60) | 19.1 ± 1.1 | 5.1 ± 1.0 | 4.1 ± 0.9 | 4.7 ± 1.1 | 4.4 ± 0.8 | 12.9 ± 1.3 | 5.7 ± 1.6 |
| | GFZ-RL05a(60) | 18.9 ± 1.1 | 4.7 ± 1.3 | 4.4 ± 1.0 | 5.5 ± 1.7 | 4.6 ± 1.0 | 14.4 ± 1.7 | 4.9 ± 1.6 |
| | AIUB-RL02(90) | 19.1 ± 1.6 | 4.3 ± 1.8 | 4.6 ± 1.6 | 5.4 ± 3.8 | 3.6 ± 4.2 | 13.9 ± 4.5 | 2.1 ± 7.3 |
| | CSR-RL05(90) | 19.9 ± 1.8 | 5.4 ± 2.3 | 4.1 ± 2.2 | 7.4 ± 3.3 | 4.8 ± 4.3 | 12.8 ± 5.1 | 3.2 ± 8.1 |
| | GFZ-RL05a(90) | 18.6 ± 2.8 | 6.7 ± 3.3 | 5.8 ± 2.7 | 2.7 ± 6.1 | 5.9 ± 5.3 | 10.2 ± 6.4 | 2.8 ± 9.5 |
| 300 km Gauss | AIUB-RL01(60) | 18.2 ± 1.1 | 4.2 ± 0.9 | 3.9 ± 0.9 | 4.6 ± 1.0 | 3.5 ± 0.8 | 12.0 ± 1.2 | 5.2 ± 1.3 |
| | AIUB-RL02(60) | 18.5 ± 1.1 | 4.5 ± 0.9 | 4.1 ± 0.8 | 4.4 ± 0.7 | 4.3 ± 0.6 | 11.9 ± 1.0 | 5.7 ± 1.1 |
| | CSR-RL05(60) | 18.3 ± 1.0 | 4.8 ± 0.9 | 3.9 ± 0.8 | 4.3 ± 0.7 | 4.3 ± 0.6 | 11.8 ± 1.0 | 5.6 ± 1.1 |
| | GFZ-RL05a(60) | 18.3 ± 1.0 | 4.6 ± 1.0 | 4.2 ± 0.8 | 4.5 ± 1.0 | 4.3 ± 0.7 | 12.2 ± 1.1 | 5.3 ± 1.1 |
| | AIUB-RL02(90) | 18.8 ± 1.1 | 4.4 ± 1.0 | 4.3 ± 0.9 | 4.6 ± 0.8 | 4.3 ± 0.7 | 12.1 ± 1.0 | 5.3 ± 1.2 |
| | CSR-RL05(90) | 18.8 ± 1.0 | 4.6 ± 0.9 | 4.1 ± 0.9 | 4.6 ± 0.7 | 4.1 ± 0.6 | 12.0 ± 1.0 | 5.4 ± 1.2 |
| | GFZ-RL05a(90) | 18.8 ± 0.9 | 4.5 ± 1.1 | 4.4 ± 0.9 | 4.8 ± 0.9 | 4.2 ± 0.7 | 12.0 ± 1.1 | 5.3 ± 1.2 |

**Table 6.** Residual RMS after removing bias, trend, annual and semi-annual variations in centimetre of equivalent water height.

| | Gravity model | Amazon | Congo | Mississippi | Nile | Jangtsekiang | Ganges | Danube |
|---|---|---|---|---|---|---|---|---|
| No smoothing | AIUB-RL01(60) | 3.6 | 3.5 | 3.7 | 4.6 | 3.4 | 5.7 | 5.6 |
| | AIUB-RL02(60) | 3.2 | 3.2 | 2.8 | 3.0 | 2.6 | 4.6 | 4.3 |
| | CSR-RL05(60) | 3.2 | 2.9 | 2.7 | 3.3 | 2.5 | 3.9 | 4.8 |
| | GFZ-RL05a(60) | 3.3 | 3.8 | 2.8 | 5.1 | 3.1 | 5.0 | 4.8 |
| | AIUB-RL02(90) | 4.6 | 5.3 | 4.5 | 10.9 | 12.1 | 12.8 | 20.9 |
| | CSR-RL05(90) | 5.2 | 6.7 | 6.2 | 9.4 | 12.3 | 14.5 | 23.1 |
| | GFZ-RL05a(90) | 7.9 | 9.4 | 7.6 | 17.4 | 15.3 | 18.3 | 27.7 |
| 300 km Gauss | AIUB-RL01(60) | 3.4 | 2.7 | 2.8 | 2.9 | 2.2 | 3.5 | 4.0 |
| | AIUB-RL02(60) | 3.2 | 2.8 | 2.5 | 2.2 | 1.9 | 3.0 | 3.4 |
| | CSR-RL05(60) | 3.1 | 2.7 | 2.4 | 1.9 | 1.8 | 2.9 | 3.4 |
| | GFZ-RL05a(60) | 2.8 | 3.0 | 2.5 | 2.8 | 2.0 | 3.3 | 3.4 |
| | AIUB-RL02(90) | 3.1 | 2.8 | 2.5 | 2.1 | 1.9 | 2.9 | 3.4 |
| | CSR-RL05(90) | 2.9 | 2.7 | 2.5 | 1.9 | 1.8 | 2.9 | 3.4 |
| | GFZ-RL05a(90) | 2.7 | 3.2 | 2.5 | 2.6 | 1.9 | 3.1 | 3.4 |

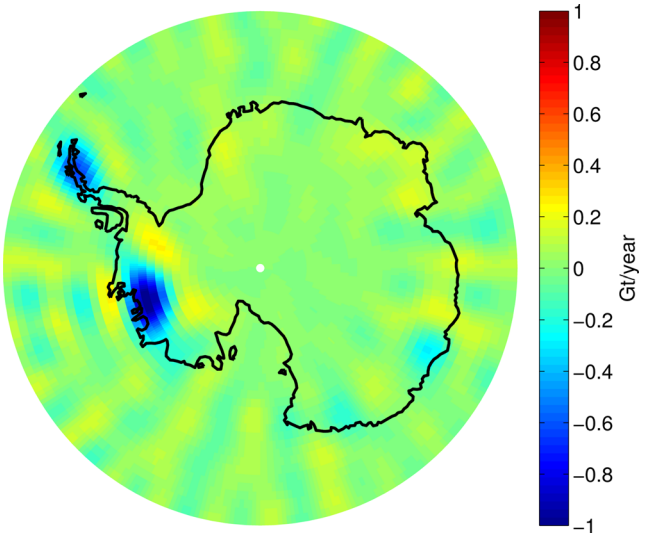


**Figure 16.** Trend estimates per 1° bin for 7 yr (2003–2009) from AIUB-RL02(60) in Antarctica. No smoothing filter was applied.

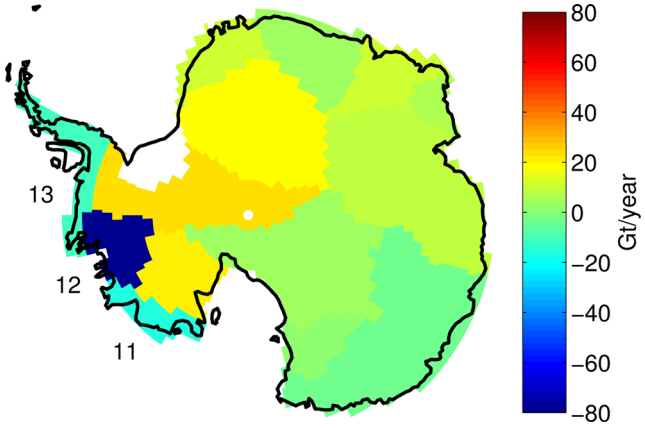


**Figure 17.** Trend estimates for 7 yr (2003–2009) from AIUB-RL02(60) in basins of Antarctica. No smoothing filter applied. Basin numbers of West coast basins are indicated.

estimates can be derived without smoothing, which is advantageous because no signal attenuation due to smoothing has to be taken into account. In case of basin 13 a large part of the basin (i.e. the Antarctic Peninsula) is oriented North-South and therefore parallel to the well-known stripes, the predominant feature of the noise in GRACE gravity fields. In this case the noise will not cancel out when computing the ice mass and smoothing becomes mandatory.

Note that the formal errors only describe the model fit and do not take into account the uncertainties in signal separation that may be introduced by a GIA-model or other error sources mentioned by Horwath & Dietrich (2009). The given amplitudes or trend estimates only serve as an illustration of the quality gain from AIUB-RL01 to -RL02 and for comparison to the official releases CSR-RL05 and GFZ-RL05a of monthly models. No precautions were taken to

**Table 7.** Linear trend estimates (Gt/year) for the three West coast basins with major mass loss and residual RMS after removing bias, linear trend, quadratic trend, annual and semi-annual variations.

| | Gravity model | Basin 11 Linear trend | Basin 12 Linear trend | Basin 13 Linear trend | Basin 11 Residual RMS | Basin 12 Residual RMS | Basin 13 Residual RMS |
|---|---|---|---|---|---|---|---|
| No smoothing | AIUB-RL01(60) | − 15.0 ± 1.1 | − 80.4 ± 2.0 | − 9.6 ± 2.7 | 17.0 | 21.3 | 41.3 |
| | AIUB-RL02(60) | − 16.6 ± 0.9 | − 78.6 ± 1.9 | − 10.4 ± 2.4 | 13.6 | 17.1 | 33.9 |
| | CSR-RL05(60) | − 15.8 ± 1.0 | − 77.6 ± 2.2 | − 8.8 ± 1.9 | 14.3 | 19.0 | 27.1 |
| | GFZ-RL05a(60) | − 18.5 ± 1.0 | − 76.8 ± 2.1 | − 14.1 ± 2.8 | 14.9 | 22.1 | 38.3 |
| | AIUB-RL02(90) | − 20.3 ± 2.0 | − 83.0 ± 3.3 | − 22.4 ± 6.5 | 28.9 | 44.4 | 93.2 |
| | CSR-RL05(90) | − 17.9 ± 2.2 | − 82.7 ± 4.0 | − 5.8 ± 11.1 | 30.4 | 55.1 | 154.5 |
| | GFZ-RL05a(90) | − 28.4 ± 3.1 | − 71.0 ± 4.7 | − 7.7 ± 12.1 | 43.1 | 57.8 | 172.2 |
| 300 km Gauss | AIUB-RL01(60) | − 11.2 ± 0.8 | − 44.4 ± 1.3 | − 9.6 ± 1.4 | 11.5 | 15.5 | 20.0 |
| | AIUB-RL02(60) | − 11.7 ± 0.6 | − 43.0 ± 1.3 | − 9.6 ± 1.4 | 8.1 | 12.6 | 16.9 |
| | CSR-RL05(60) | − 11.0 ± 0.6 | − 42.9 ± 1.4 | − 9.9 ± 1.1 | 8.6 | 13.0 | 13.1 |
| | GFZ-RL05a(60) | − 12.5 ± 0.6 | − 42.1 ± 1.4 | − 11.0 ± 1.4 | 8.2 | 14.3 | 18.3 |
| | AIUB-RL02(90) | − 12.0 ± 0.6 | − 43.9 ± 1.4 | − 10.0 ± 1.4 | 8.2 | 12.2 | 17.2 |
| | CSR-RL05(90) | − 11.3 ± 0.6 | − 43.6 ± 1.5 | − 9.7 ± 1.1 | 8.5 | 12.8 | 13.1 |
| | GFZ-RL05a(90) | − 12.4 ± 0.6 | − 42.1 ± 1.4 | − 10.6 ± 1.6 | 8.7 | 14.1 | 19.2 |

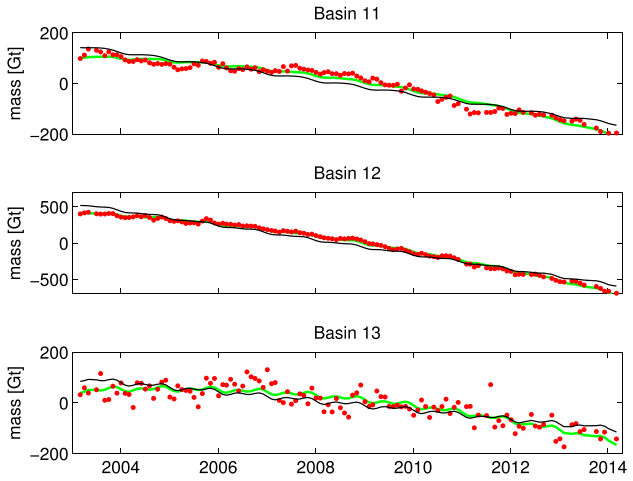


**Figure 18.** Mass estimates for three basins at the west coast of Antarctica. Red: monthly mass estimates, black: model including linear trend and seasonal variations, green: model including quadratic trend and seasonal variations. No smoothing was applied.

take spectral leakage into account or to compensate attenuation by smoothing.

## 6 SUMMARY AND OUTLOOK

The availability of reprocessed GRACE L1B-data and updated background models asked for a reprocessing of monthly GRACE gravity models AIUB-RL01. The opportunity was taken to also switch to new GPS orbits based on IERS2010 conventions, to implement the application of shallow ocean-tides, and to review the parametrization.

The reprocessing led to an important reduction in noise and an enhanced estimability of seasonal and secular gravity variations. The time-series of monthly models moreover was extended to the time interval from March 2003 to March 2014. AIUB-RL02 is available in two versions, one up to degree and order 90, the other up to degree and order 60. During periods of orbit resonance or increased solar activity it is recommended to use AIUB-RL02(60).

A major improvement is due to the estimation of daily accelerometer scale factors which drastically reduce spurious signal at the 161 d period in low degree coefficients, especially in $C_{20}$. This reduction is in particular important during periods of high solar activity.

Further improvement may result by an improved noise model and an observation dependent weighting. Both measures are planned to be implemented and tested within the frame of the EGSIEM project. The as yet unexplained tension between the GPS and K-Band measurements, reduced either by downsampling or downweighting GPS is a key difficulty in this context.

Compared to CSR-RL05 or GFZ-RL05a, the new AIUB-RL02 time-series stand out by their low noise, in particular for the high degrees. AIUB-RL02 therefore will be of special interest for all users wishing to analyse signals beyond what is left by the commonly used 300 km Gauss filter. AIUB-RL02 can be downloaded from ftp://ftp.unibe.ch/aiub/GRAVITY/GRACE (last accessed 22 March 2016).

An additional advantage of the AIUB gravity fields processed by the CMA is their unbiasedness because they are to a large extent independent of the choice of the *a priori* gravity model. When comparing the full range of monthly models available at ICGEM, AIUB-RL02 turns out to be closest to their arithmetic mean, thus supporting their unbiasedness. The comparison and combination of monthly models from different processing centres is part of the EGSIEM project and will be the topic of a separate publication (Jean *et al.*, in preparation).

## ACKNOWLEDGEMENTS

Our thanks go to Torsten Mayer-Gürr for his substantial assistance with the implementation of the model of shallow ocean tides and to Christoph Dahle for providing the internal version of GFZ-RL05a, which was estimated with reduced degree and order 60. This project received funding from the European Union's Horizon 2020 research and innovation program under grant agreement No. 637010. This paper reflects only the authors' view. The Research Executive Agency is not responsible for any use that may be made of the information it contains.

## REFERENCES

Altamimi, Z., Collilieux, X. & Métivier, L., 2011. ITRF2008: an improved solution of the international terrestrial reference frame, *J. Geod.*, **85,** 457–473.

Bettadpur, S., 2012. CSR level-2 processing standards document for level-2 product release 0005. GRACE 327-742.

Beutler, G., Jäggi, A., Mervart, L. & Meyer, U., 2010a. The celestial mechanics approach: theoretical foundations, *J. Geod.,* **84,** 605–624.

Beutler, G., Jäggi, A., Mervart, L. & Meyer, U., 2010b. The celestial mechanics approach: application to data of the GRACE mission, *J. Geod.,* **84,** 661–681.

Chambers, D.P. & Bonin, J.A., 2012. Evaluation of Release 05 time-variable gravity coefficients over the ocean, *Ocean Science,* **8,** 859–868.

Chen, J.L., Wilson, C.R. & Tapley, B.D., 2010. The 2009 exceptional Amazon flood and interannual terrestrial water storage change observed by GRACE, *Water Resour. Res.,* **46,** 12526, doi:10.1029/2010WR009383.

Dach, R. *et al.*, 2009. GNSS processing at CODE: status report, *J. Geod.,* **83,** 353–366.

Dahle, C., Flechtner, F., Gruber, C., König, D., König, R., Michalak, G. & Neumayer, K. H., 2012. GFZ GRACE Level-2 Processing Standards Document for Level-2 Product Release 0005. Scientific Technical Report STR12/02 – Data, Revised Edition, January 2013, Potsdam, doi:10.2312/GFZ.b103-1202-25.

Davis, J.L., Tamisiea, M.E., Elósegui, P., Mitrovica, J.X. & Hill, E.M., 2008. A statistical filtering approach for Gravity Recovery and Climate Experiment (GRACE) gravity data, *J. geophys. Res.,* **113,** B04410, doi:10.1029/2007JB005043.

Dunn, C.E. *et al.*, 2003. Instrument of GRACE: GPS augments gravity measurements, *GPS World,* **14,** 16–28.

Flechtner, F. & Dobslaw, H., 2013. AOD1B Product Description Document for Product Release 05. GRACE Project Document JPL 327-750, Version 4.0, Available at: http://isdc.gfz-potsdam.de/grace, last accessed 22 March 2016.

Hartmann, T. & Wenzel, H., 1995. The HW95 tidal potential catalogue, *Geophys. Res. Lett.,* **22,** 3553–3556.

Horwath, M. & Dietrich, R., 2009. Signal and error in mass change inferences from GRACE: the case of Antarctica, *Geophys. J. Int.,* **177,** 849–864.

Horwath, M., Lemoine, J.M., Biancale, R. & Bourgogne, S., 2011. Improved GRACE science results after adjustment of geometric biases in the Level-1B K-band ranging data, *J. Geod.,* **85,** 23–38.

Jäggi, A., Hubentobler, U. & Beutler, G., 2006. Pseudo-stochastic orbit modeling techniques for low-Earth orbiters, *J. Geod.,* **80,** 47–60.

Jäggi, A., Dach, R., Montenbruck, O., Hugentobler, U., Bock, H. & Beutler, G., 2009. Phase center modeling for LEO GPS receiver antennas and its impact on precise orbit determination, *J. Geod.,* **83,** 1145–1162.

Jäggi, A., Beutler, G. & Mervart, L., 2010. GRACE gravity field determination using the celestial mechanics approach—first results, in *Gravity, Geoid and Earth Observation,* pp. 177–184, ed. Mertikas, S.P., International Association of Geodesy Symposia 135.

Jäggi, A., Beutler, G., Meyer, U., Prange, L., Dach, R. & Mervart, L., 2011a. AIUB-GRACE02S: status of GRACE gravity field recovery using the celestial mechanics approach, in *Geodesy for Planet Earth,* pp. 161–170, eds Kenyon, S., Pacino, M.C. & Marti, U., International Association of Geodesy Symposia 136, doi:10.1007/978-3-642-20338-1_20.

Jäggi, A., Prange, L. & Hugentobler, U., 2011b. Impact of covariance information of kinematic positions on orbit reconstruction and gravity field recovery, *Adv. Space Res.,* **47,** 1020–1028.

Jäggi, A. *et al.*, 2015. European Gravity Service for Improved Emergency Management - a new Horizon 2020 project to serve the international community and improve the accessibility to gravity field products, in *EGU General Assembly 2015,* Vienna, Austria, 12–17 April.

Long, D., Scanlon, B.R., Longuevergne, L., Sun, A.Y., Fernando, D.N. & Save, H., 2013. GRACE satellite monitoring of large depletion in water storage in response to the 2011 drought in Texas, *Geophys. Res. Lett.,* **40,** 3395–3401.

Lyard, F., Lefevre, F., Letellier, T. & Francis, O., 2006. Modelling the global ocean tides: modern insights from FES2004, *Ocean Dyn.,* **56,** 394–415.

Mayer-Gürr, T., Savcenko, R., Bosch, W., Daras, I., Flechtner, F. & Dahle, Ch., 2011. Ocean tides from satellite altimetry and GRACE, *J. Geodyn.,* **59,** 28–38.

McCarthy, D.D. & Petit, G. (eds), 2003. IERS Conventions (2003). International Earth Rotation and Reference Systems Service (IERS), IERS Technical Note No. 32, Verlag des Bundesamtes für Karthographie und Gedäsie, Frankfurt am Main.

Meyer, U., Jäggi, A. & Beutler, G., 2012. Monthly gravity field solutions based on GRACE observations generated with the Celestial Mechanics Approach, *Earth planet. Sci. Lett.,* **345,** 72–80.

Meyer, U., Jäggi, A., Beutler, G. & Bock, H., 2015a. The impact of common versus separate estimation of orbit parameters on GRACE gravity field solutions, *J. Geod.,* **89,** 685–696.

Meyer, U., Dahle, C., Sneeuw, N., Jäggi, A., Beutler, G. & Bock, H., 2015b. The effect of pseudo-stochastic orbit parameters on GRACE monthly gravity fields – insights from lumped coefficients, in Sneeuw *et al.* (eds), VIII Hotine-Marussi Symposium on Mathematical Geodesy, International Association of Geodesy Symposia 142, doi:10.1007/1345_2015_67.

Petit, G. & Luzum, B. (eds), 2010. IERS Conventions (2010). International Earth Rotation and Reference Systems Service (IERS), IERS Technical Note No. 36, Verlag des Bundesamtes für Karthographie und Gedäsie, Frankfurt am Main.

Savcenko, R. & Bosch, W., 2011. EOT11a—a new tide model from Multi-Mission Altimetry, in *OSTST Meeting,* San Diego, 19–21 October.

Schmidt, R. *et al.*, 2007. GRACE time-variable gravity accuracy assessment, in *Dynamic Planet*, pp. 237–243, eds Tregoning, P. & Rizos, C., International Association of Geodesy Symposium 130, Springer.

Seo, K.W., Wilson, C.R., Chen, J. & Waliser, D.E., 2008. GRACE's spatial aliasing error, *Geophys. J. Int.,* **172,** 41–48.

Steigenberger, P., Lutz, S., Dach, R. & Hugentobler, U., 2011. CODE Contribution to the First IGS Reprocessing Campaign. Technical Report.

Swenson, S. & Wahr, J., 2002. Methods for inferring regional surface-mass anomalies from Gravity Recovery and Climate Experiment (GRACE) measurements of time-variable gravity, *J. geophys. Res.,* **107,** B92193, doi:10.1029/2001JB000576.

Tapley, B.D., Bettadpur, S., Ries, J.C., Thompson, P.F. & Watkins, M., 2004. GRACE measurements of mass variability in the Earth system, *Science,* **305**(5683), 503–505.

Velicogna, I., 2009. Increasing rates of ice mass loss from the Greenland and Antarctic ice sheets revealed by GRACE, *Geophys. Res. Lett.,* **36,** 19503, doi:10.1029/2009GL040222.

Wahr, J., Molenaar, M. & Bryan, F., 1998. Time variability of the Earth's gravity field: hydrological and oceanic effects and their possible detection using GRACE, *J. geophys. Res.,* **103,** 30 205–30 230.

Watkins, M. & Yuan, D.N., 2012. JPL Level-2 Processing Standards Document, For Level-2 Product Release 05.